ILC Beam Energy Measurement Using Compton Backscattering

N. Muchnoi[1], H.J. Schreiber[2] and M. Viti[2]

1- Budker Institute for Nuclear Physics BINP
Novosibirsk 630090 - Russian Federation

2- Deutsches Elektronen-Synchrotron DESY
15738 Zeuthen, Germany

An alternative approach to measure the ILC beam energy is suggested. Beam electrons interact with monochromatic laser light so that downstream of the interaction point unscattered beam particles (most of them) and strongly collimated Compton backscattered electrons and photons exist. After passing a dipole, these particles are divided into non-deflected high energy photons, less deflected beam particles and scattered electrons with some larger deflection. Measuring the spatial distributions of these types of particles permits to infer the beam energy with an accuracy 10^{-4} or better. Since the systematics of the Compton backscattering approach are quite different from those of the BPM-based energy spectrometer, Compton backscattering provides an independent beam energy calibration system with comparable accuracy. The approach has no strict limitations on the beam energy, so it might be experimentally tested at lower energy machines.

1 Introduction

Accurate knowledge of the energy of colliding beams plays an important role in the physics program of the ILC. For example, masses of particles can be precisely determined either by means of threshold scans of cross sections of pair produced particles or by improving the 4-momenta of particles produced in the continuum. At circular lepton colliders the energy scale was accurately calibrated by means of the resonant depolarization technique, which is however not applicable at linear colliders. So at linear colliders some new approaches for beam energy monitoring are needed to be addressed.

Compton backscattering of monochromatic laser light on beam particles permits access to the beam energy utilizing precise information of the Compton backscattered electrons and photons. This approach is thought to be complementary to the canonical method of beam position monitor (BPM)-based magnetic spectrometers [2]. In the past, Compton backscattering has been applied to perform precise beam energy measurements at low energy storage rings such as BESSY-I, BESSY-II (Berlin) [3], the Taiwan Light Source [4] and the VEPP-4M collider (Novosibirsk) [5].

2 Outline of the experiment

A sketch of the scheme suggested for beam energy monitoring at the ILC is shown in Fig, 1. Beam electrons collide with monochromatic laser radiation at some small angle α. Downstream of the laser-electron interaction point (IP) non-interacting beam particles (most of them), Compton scattered electrons and photons are strongly collimated in the forward direction. A dipole magnet separates them into through-going high-energy photons, less deflected beam electrons and scattered electrons with some larger deflection. If a photon

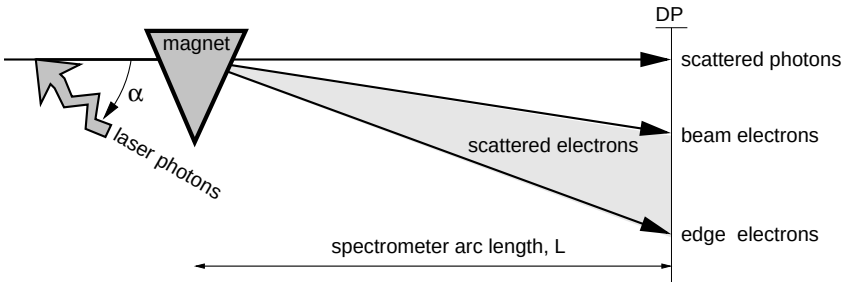

Figure 1: Sketch of the beam energy monitoring scheme at the ILC.

with energy ω_L is scattered head-on with a relativistic electron of energy ε (or E_{beam}) at some small angle α, the maximum energy of the scattered photon is

$$\omega_{max} = \frac{\varepsilon^2}{\varepsilon + \dfrac{m^2}{4\omega_0}} , \qquad \text{where } \omega_0 = \omega_L \cos^2(\alpha/2) . \tag{1}$$

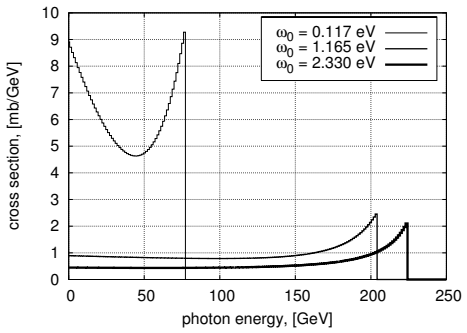

Figure 2: Backscattered photon energy spectra for three laser energies ω_0, ε=250 GeV and α=8 mrad.

These photons are scattered exactly along the momentum of the incident electron[a]. Fig. 2 shows the Compton cross section as a function of the energy of backscattered photons for three laser energies. Photons with energy ω_{max} form a sharp high energy edge, which is mirrored by energy conservation to the electron energy spectrum as shown in Fig. 3. Electrons with minimum energy, given by $\varepsilon + \omega_L - \omega_{max}$, are called edge electrons and their energy is related to the beam energy ε via

$$E_{edge} = \frac{\varepsilon}{1 + \dfrac{4\varepsilon\omega_0}{m^2}} . \tag{2}$$

If monochromatic laser light scatters with beam electrons, the luminosity of the

[a]That is the reason of taking about Compton backscattering.

Compton process can be adjusted such that only a small fraction of the beam particles interact and the scattered photons, respectively, electrons posses a clear step-like peculiarity in their respective energy spectrum, from which ω_{max}, respectively, E_{edge} can be inferred. The relation of ω_{max} or E_{edge} with the beam energy, given by (1) respectively (2), permits then to extract the incident electron energy. However, precise spectrometry of the beam energy at the ILC is still challenging because, as seen from Figs. 2 and 3, Compton backscattered particles have frequently energies close to E_{beam}.

After passing the B-field of the spectrometer magnet, the deflection range of the scattered electrons has to be smaller than the magnet pole length, so that both the beam as well as the Compton electrons 'see' the same B-field integral $\int Bdl$. The amount of deflection is given by the bending angle, which in turn is inverse proportional to the particle's energy E

$$\theta(E) \sim \frac{\int Bdl}{E} + \delta_{SR} \,, \qquad (3)$$

where δ_{SR} is a small correction term from synchrotron radiation. It can be shown that $\delta_{SR} \sim (\int Bdl)^3$ and does not depend on the particle energy E. In this study we neglect synchrotron radiation effects. However, detailed simulation studies should account for this correction.

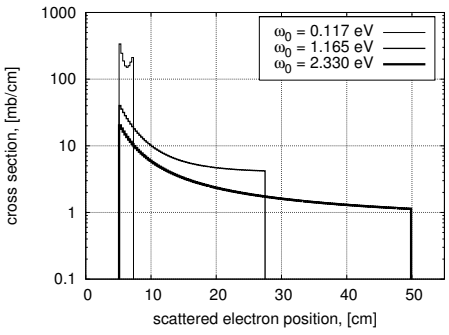

Figure 4: Scattered electrons distribution in the DP for three ω_L values, ε=250 GeV, an arc length of L=48.5 m, and a perfect 3 m long magnet with B=0.28 T.

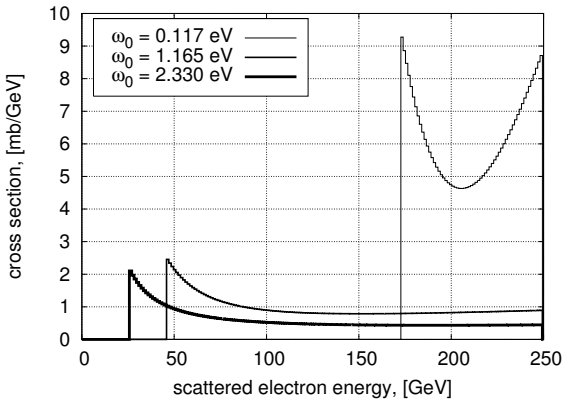

Figure 3: Scattered electron energy spectra for three laser energies ω_0, ε=250 GeV and α=8 mrad.

After the magnet all particles propagate in free space of length L (spectrometer arc length) up to the detector plane (indicated as DP in Fig. 1). In our setup, θ is in the order of some millirad and therefore the electron transverse position in the detector plane is approximated by

$$X(E) = X_0 + A/E \,, \qquad (4)$$

where $A \sim L \cdot \int Bdl$ and X_0 the non-deflected photon position, determined by the center-of-gravity of the backscattered photons.

Fig. 4 represents the position range of backscattered electrons at the detector plane for 250 GeV beam particles and three laser energies. The electrons cover the distance between the beam position $X_{beam} = X(E_{beam})$ and that of the edge electrons $X_{edge} = X(E_{edge})$, where the cut-off energy of the edge electrons is directly transformed into a sharp edge location.

According to eqs.(2) and (4), $X(E_{beam})$ and $X(E_{edge})$ can be expressed as

$$X_{beam} \equiv X(E_{beam}) = X_0 + A/E_{beam} \tag{5}$$

$$X_{edge} \equiv X(E_{edge}) = X_{beam} + A\frac{4\omega_0}{m^2} \tag{6}$$

and hence the beam energy can be deduced from

$$E_{beam} = \frac{m^2}{4\omega_0} \cdot \frac{X_{edge} - X_{beam}}{X_{beam} - X_0} \ . \tag{7}$$

Thus, E_{beam} can be determined from the electron rest mass m, the well-known laser energy ω_L and three particle positions which have to be deduced from the experiment: X_0, X_{beam} and X_{edge}. The beam position X_{beam} can be measured by a high resolution BPM, while monitoring the positions of the edge electrons X_{edge} and the photon center-of-gravity X_0 needs dedicated high spatial resolution detectors. X_{edge} can e.g. be obtained from the position distribution of backscattered electrons via fitting the edge spectrum similar to the photon energy spectrum as performed at the VEPP-4M collider [5] using a HPGe detector, see Fig. 5.

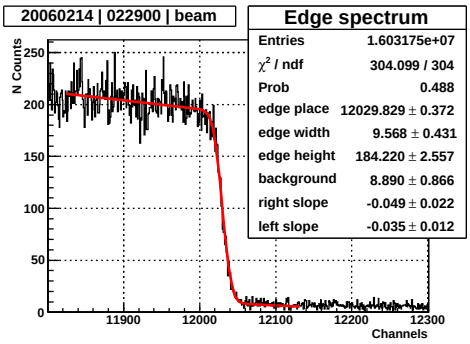

Figure 5: Compton backscattered photon energy spectrum measured by 120 ml HPGe detector at the VEPP-4M collider ($\simeq$0.5 keV/ch)

It is important to mention that within this scheme precise beam energy measurements do not require precise knowledge of the absolute B-field integral. This is in contrast to the approach of measuring E_{beam} directly from the energy of the edge electrons, where absolute field integral information of the spectrometer magnet must exist with high precision.

The error of the beam energy, which has to be monitored with $\Delta E_{beam}/E_{beam} \lesssim 10^{-4}$, can be estimated from eq.(7) as

$$\frac{\Delta E_{beam}}{E_{beam}} = \frac{X_{edge}}{X_{edge} - X_{beam}}\left(\frac{\Delta X_{edge}}{X_{edge}}\right) \oplus \frac{X_{edge}}{X_{edge} - X_{beam}}\left(\frac{\Delta X_{beam}}{X_{beam}}\right) \oplus \frac{\Delta X_0}{X_{beam}} \ . \tag{8}$$

For the particular set of spectrometer parameters as used in Fig. 4, X_{beam} turns out to be close to 5 cm, and to achieve $\Delta E_{beam}/E_{beam}$ better than 10^{-4}, X_{beam} and X_0 (see also the last two terms in eq.(8)) have to be determined with accuracy of about 3 μm.

The precision of X_{Edge} can be evaluated from the number of scattered electrons near the edge and the width of the edge, $\sigma_{X_{edge}}$. A non-zero edge width is supposed to be caused by several effects of which the most important ones are internal energy and angular spreads of the beam particles at the Compton IP. Such effects, which cause $\sigma_{X_{edge}}$ to be finite, define together with the statistics, the precision of X_{Edge} as

$$\Delta X_{edge} = \sqrt{\frac{2 \cdot \sigma_{X_{edge}}}{\frac{dN}{dx}(X_{edge})}} \ . \tag{9}$$

The behaviour of the first term in eq.(8) is shown in Fig. 6 against the beam energy for three laser types. Here, the following assumptions were made: a) the number of Compton events per bunch crossing is 10^6, b) the electron detection efficiency is 100%, c) the B-field integral is linear proportional to the beam energy enabling X_{beam} to be independent on E_{beam} and d) smearing of X_{edge} is mainly caused by the angular spread of the electrons, which was assumed of 5 mrad. It can be noticed that, within the assumptions made, beam energy uncertainties of better than 10^{-4} are achievable, and lasers with short wavelengths are prefered. In particular, the 1.165 eV line of an infrared laser is much better suited then the far-infrared CO_2 laser.

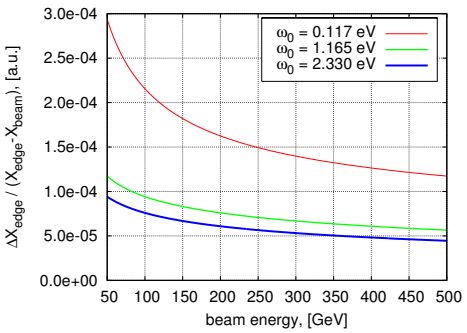

Figure 6: Precision of X_{edge} versus the beam energy for three laser energies..

Generation of 10^6 Compton scatters from $2 \cdot 10^{10}$ electrons per ILC bunch requires however a $Nd:YAG$ laser of typically 10 ps pulse duration and a pulse power of 20 mJ to be focused to a spot size of $\sim$50 μm at the Compton IP [6], as an example. Such a laser that matches the pattern of the ILC bunches with sufficient pulse power is at present commercially not available, hence further R&D is needed. It has also been shown in [6] that multiple scattering and non-linear corrections within the Compton process are of no concern, despite the large laser power required.

More details on precisions of the beam energy on statistics, which is to a large extent controlled by ΔX_{edge}, respectively, the first term in eq.(8), can be deduced from Fig. 7. Here, $\frac{\Delta X_{edge}}{X_{edge}-X_{beam}}$, which is the only statistics dependent term in (8), is shown against the

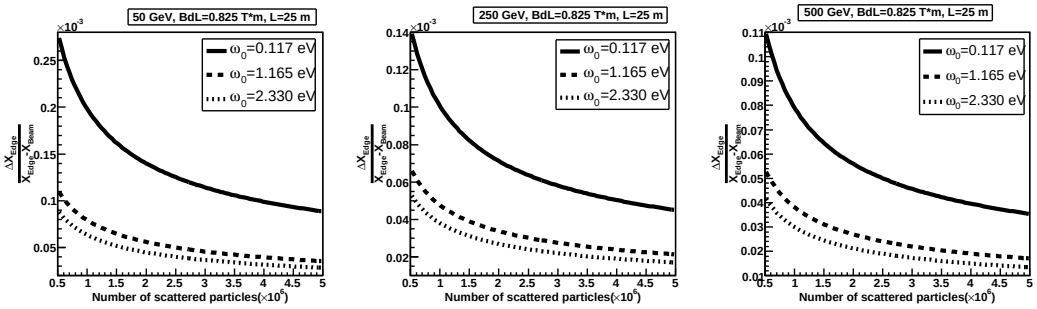

Figure 7: The first term of eq.(8) as a function of the number of Compton events ($\times 10^6$) per bunch crossing for three beam and laser energies.

number of Compton events per bunch crossing. These numbers were derived assuming a) the beam spot size is 50 μm at the detector plane in x and y, b) the internal energy spread is 0.15%, c) the accuracies on beam position and photon center-of-gravity are both 1 μm and the field integral equals $\int Bdl = 0.84$ Tm. One notices, for event rates less than 10^6 some improvements of $\frac{\Delta E_{beam}}{E_{beam}}$ can be achieved by maintaining larger event rates. This is

mostly evident for a CO_2 laser. Event rates beyond a few millions would have however less or negligible impact for better uncertainties of the beam energy. Whether such large event rates per bunch crossing can be realized depends mainly on ongoing laser developments.

On the other hand, even if we intend to measure the energy of each ILC bunch, there is no need to adjust the Compton luminosity or the laser power for 10^6 events per bunch crossing. From eqs.(6) and (7) follows that the numerator in eq.(7), $X_{edge} - X_{beam}$, is only coupled to spectrometer parameters such as the B-field integral and the drift distance L, and does not depend on the beam energy. Since bunch-to-bunch energy variations are supposed to proceed rapidly and spectrometer parameters change at a much larger timescale, we might, for each bunch, record the beam position X_{beam} and the position spectrum of electrons close to the edge. Accumulating these informations over many bunches provides a precise $X_{edge} - X_{beam}$ value, which is not rendered by insufficient bunch related Compton events. However, the denominator in eq.(7), $X_{beam} - X_0$, has to be measured for each bunch crossing, which can be performed by a high resolution BPM and, because of the large backscattered photon yield, by a precise center-of-gravity position device.

3 Spectrometer locations within the Beam Delivery System

In order to locate the spectrometer within the Beam Delivery System (BDS) [7] some basic constraints have to be accounted for. These constraints are caused by physics arguments related to systematical and statistical errors of each component of the spectrometer, additional background from Compton electron interactions with downstream magnets as well as space limitations within the BDS. In this section some pros and cons of possible locations of the Compton spectrometer within the BDS are shortly discussed.

3.1 Practical restrictions

In order to measure Compton backscattered electrons and photons, they have to leave the vacuum chamber, assumed to be a pipe of 20 mm diameter. This constrains the B-field integral $\int BdL$ and the drift distance L between the magnet and the detector plane.

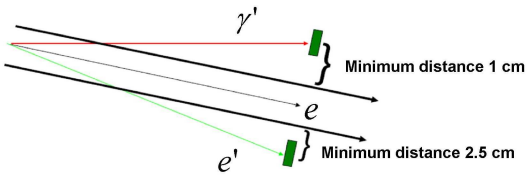

Figure 8: Illustration of spacing requirements at the detector plane.

According to eq.(4), the space between the center-of-gravity of the backscattered photons and the beamline as well as between the edge electrons and the beam depends on the parameter A, which is proportional to the product $A \sim L \cdot \int Bdl$.

Therefore, A might be changed either by B-field or drift distance L variations, or both simultaneously. For the moment we fix $\int Bdl$ such that the bending angle for beam particles is 1 mrad and allow L to vary. For the sake of illustration the minimum distance between the beam pipe wall and the center of the photon detector should be, for practical reasons, in the order of 10 mm, while the center of the electron detector might be 25 mm away from the wall as illustrated in Fig. 8. These numbers should not be considered as strict, but thought to indicate the space requirements for reasonable particle position measurements. Since the distance to the electron detector is not really a concern, the location of the photon detector being only 20 mm off the beam

needs special care. Accepting these numbers, a 3 meter long magnet with a B-field of 0.28 T (corresponding to $\int Bdl$=0.84 Tm) combined with a drift distance of 20 m ensures such minimal separations.

The dependence of the first term in eq.(8), $\frac{\Delta X_{edge}}{X_{edge}-X_{beam}}$, as a function of L is displayed in Fig. 9 for three beam and laser energies.

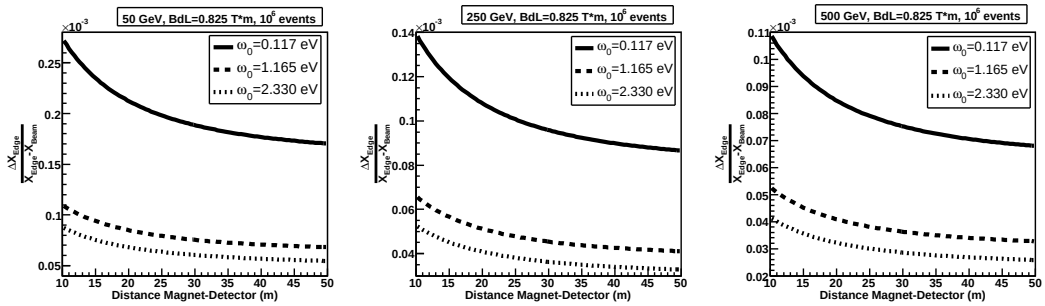

Figure 9: The first term of eq.(8) against drift distance L for three beam and laser energies.

Clearly, $\frac{\Delta X_{edge}}{X_{edge}-X_{beam}}$ does not strongly dependent on L, especially for high energy lasers, provided the drift distance is at least 20 m. The dependence becomes somewhat more pronounced when the spot size of the beam at the detector plane is substantially larger than 50 μm assumed so far.

Since A is proportional to the product $L \cdot \int Bdl$, it is totally equivalent to keep either $\int Bdl$ constant and to vary L or the opposite. An increase of the B-field has however carefully studied because additional beam emittance dilution has to be limited.

Last not least, Fig. 10 shows the beam energy uncertainty $\frac{\Delta E_{beam}}{E_{beam}}$ as a function of ΔX_{edge}, where ΔX_{edge} should be now understood as the total error of the electron edge position.

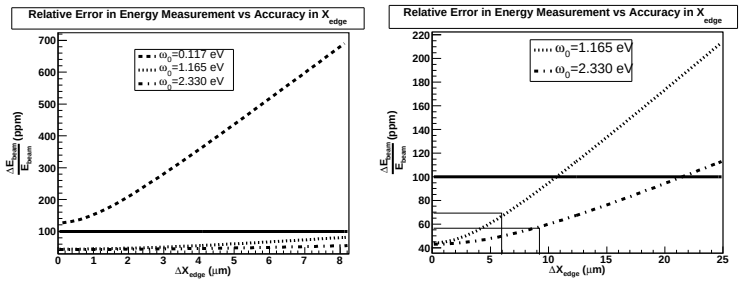

Figure 10: Left: $\frac{\Delta E_{beam}}{E_{beam}}$ as a function of ΔX_{edge} for three laser energies. Right: zoom of the left-hand figure for two laser energies. The horizontal line indicates the precision limit of a 100 ppm beam energy error.

The left part of Fig. 10 reveales that using a CO_2 laser $\frac{\Delta E_{beam}}{E_{beam}}$ rises strongly with increasing ΔX_{edge}. But more important is the error of the beam energy at $\Delta X_{edge} = 0$,

i.e. for perfect edge position information. This error exceeds 10^{-4}, respectively, 100 parts per million (ppm), which means a CO_2 laser should not be considered as an option for the proposed Compton spectrometer. Employing an Nd:YAG infrared or green laser is much more suitable as seen in the right-hand side of Fig. 10. In particular, for an infrared laser ($\omega_0 = 1.165$ eV) a 6 μm uncertainty on ΔX_{edge} provides a beam energy uncertainty of 66 ppm. To keep the uncertainty of the incident energy at 100 ppm, ΔX_{edge} has to be known with 10 μm. A green laser ($\omega_0 = 2.33$ eV) allows somewhat to relax this constraint.

Tab. 1 summarizes, for a laser with $\omega = 1.165eV$, the individual error terms of eq.(8) utilizing a spectrometer magnet with 1 mrad beam bending power. The uncertainties shown assume for ΔX_{edge}, ΔX_{beam} and ΔX_0 6 μm, 1 μm and 1 μm, respectively.

Beam Energy (GeV)	50		250		500	
Distance L (m)	25	50	25	50	25	50
$\frac{X_{edge}}{X_{edge}-X_{beam}}\left(\frac{\Delta X_{edge}}{X_{edge}}\right)$ (ppm)	79	68	46	41	38	33
$\frac{X_{edge}}{X_{edge}-X_{beam}}\left(\frac{\Delta X_{beam}}{X_{beam}}\right)$ (ppm)	80	40	46	24	42	22
$\frac{\Delta X_0}{X_{beam}}$ (ppm)	40	20	40	20	40	20

At E_{beam}= 50 GeV, accuracy of the beam energy results to 119 ppm for $L = 25$ m, whereas it is reduced to 66 ppm at 250 GeV beam energy. These numbers show that as long as L is larger or close to 25 m no restrictions would exist to perform beam energy measurements with 100 ppm or better precision. Furthermore, drift distances of $L \geq 25$ m also ensure sufficient large separation of the Compton backscattered photons from the beamline.

3.2 Possible locations within the BDS

Although the today's beam delivery system [7] is believed to be further developed within the next years, basic properties are assumed to be unchanged. We propose three alternatives for possible locations of the Compton spectrometer, but keeping major design parameters unaltered.

An overall view of the BDS is shown in Fig. 11, where also potential locations for the Compton spectrometer are indicated.

Common to all alternatives is the demand to locate the spectrometer upstream of the energy collimation system[b] in order to avoid large background (muons) excess to the expected background from normal collimation losses [8].

The straight-forward approach suggests to locate the spectrometer into a sufficient free-space region within the BDS. The amount of space needed, of the order of 60-70 m, is determined by the 25 m long drift space together with the spectrometer magnet plus at least two ancillary magnets to compensate the bending of the spectrometer dipole and the drift spaces between them. Very upstream of the e^+e^- IP, such free space exists, see Fig. 11. Whether however the addition of new bends increases the beam emittance to non-tolerable values has to be checked. First estimates indicate an emittance dilution of about 0.5% for a 250 GeV beam.

[b] This system performs efficient removal of halo particles which lie outside the acceptable range of energy spread.

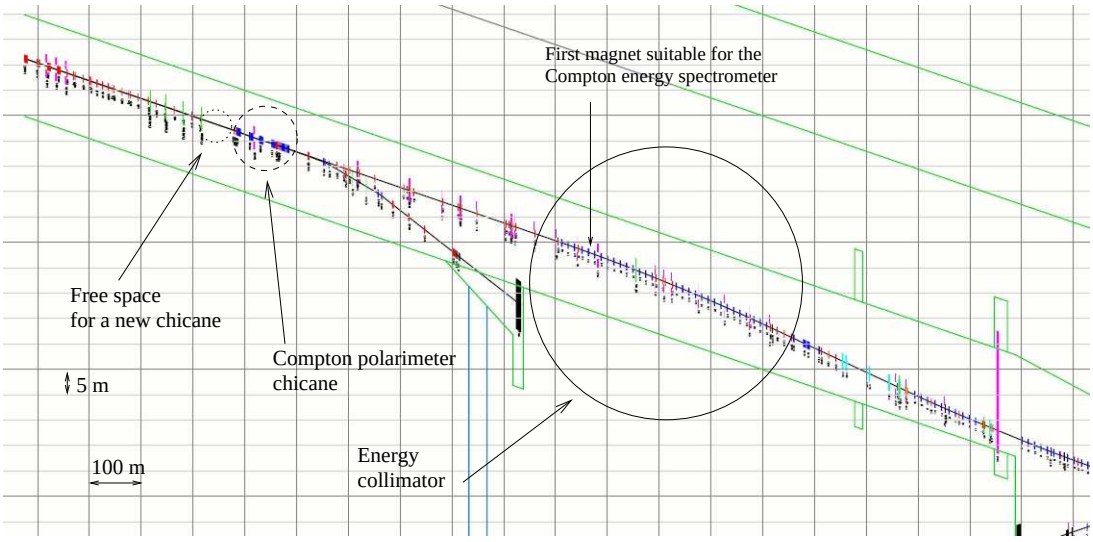

Figure 11: Scheme of the BDS with possible locations of the Compton spectrometer.

A suitable alternative for the spectrometer location consists in employing magnets of the present BDS for the spectrometer. At the beginning of the energy collimation section (see Fig. 11) several magnets[c] might be combined to provide the desired bending power. In particular, such a combination of magnets would provide sufficient particle separation if the laser IP is e.g. located before the magnet marked in Fig 11. After passing magnet 6 in the chain, separation between Compton backscattered γ-rays and the beamline becomes 18 mm, while the distance of the beamline to the edge electrons, being laser dependent, is 98 mm for an infrared laser ($\omega_0 = 1.165$ eV). Thus, by locating the detector close to magnet 7 convenient position measurements for all particle species can be performed. Since this alternative does not require additional magnets, any further beam emittance growth is a priori avoided. However, the aperture of the magnets integrated into the system has to be continuously increased towards the bending direction allowing the edge electrons to pass in B-fields with properties as demanded. For example, at the exit of magnet 6 the uniformity of the B-field should extend up to about 100 mm in the bending direction.

The third option for a Compton spectrometer location consists in employing the magnetic chicane proposed for high energy polarization measurements [9]. In particular, the four magnets of the polarimeter chicane with its laser IP in the mid-point is proposed to be supplemented by a second IP for E_{beam} measurements, which is either located upstream of the first magnet or in between the first and second magnet. However, whether both measurements can be merged into one common concept needs dedicated studies.

[c]Each magnet has a B-field of 291.68 Gauss, a length of 2.4 m and space in between of 12.3 m.

4 Summary

The BPM-based energy spectrometer [2] now under investigation is considered as the primary tool for accurate ILC beam energy monitoring. But experiences from LEP and SLD emphasize that more than one technique should be employed for precise $\sqrt{s}$ determination and cross-calibration of absolute energy data is mandatory. Therefore, a new approach to perform beam energy measurements is suggested in this study. A spectrometer utilizing Compton backscattering of laser light on beam electrons seems to provide precisions for E_{beam} of 10^{-4} or better, on a bunch-to-bunch basis without beam disruption. Properties of such a spectrometer are discussed with the conclusion that no serious performance limitations are visible.

More details on the proposed Compton energy spectrometer will appear in a forthcoming paper [10].

References

[1] Slides:
`http://ilcagenda.linearcollider.org/contributionDisplay.py?contribId=179&sessionId=78&confId=1296`.
`http://ilcagenda.linearcollider.org/contributionDisplay.py?contribId=180&sessionId=78&confId=1296`.

[2] V.N. Duginov et al., *The Beam Energy Spectrometer at the International Linear Collider*, LC-DET-2004-031 (2004).

[3] R. Klein *et al.* Nucl. Instrum. Meth. **A384** 293 (1997);
R. Klein *et al.* Nucl. Instrum. Meth. **A486** 545 (2002).

[4] Ian C. Hsu, Cha-Ching Chu and Chuang-Ing Yu, Phys. Rev. **E54** 5657 (1996).

[5] N. Muchnoi, S. Nikitin and V. Zhilich, *Fast and Precise Beam Energy Monitor Based on the Compton Backscattering at the VEPP-4M Collider*,
Proceedings of EPAC06, Edinburgh, Scotland, 26-30 Jun 2006
`http://accelconf.web.cern.ch/AccelConf/e06/PAPERS/TUPCH074.PDF`.

[6] H.J. Schreiber, *Compton Backscattering as a Tool for Precise Beam Energy Measurement*,
`http://ilcagenda.linearcollider.org/contributionDisplay.py?contribId=30&sessionId=26&confId=1049`.

[7] A. Seryi et al. Proceedings of PAC07, Albuquerque, New Mexico, USA, June 25-29, 2007;
ILC BDS lattice online repository: `http://www.slac.stanford.edu/mdw/ILC/2006e/.`

[8] L. Keller, private communication.

[9] N. Meyners, V. Gharibyan and K.P. Schüler, Proceedings of the 2005 Internationale Linear Collider Workshop, p. 871, Stanford, California, USA, 18-22 March, 2005;
K.O. Eyser, these Proceedings.

[10] N. Muchnoi, H.J. Schreiber and M. Viti, in preparation.